

Microscopic calculation of \bar{K} atomic and Λ^* hypernuclear carbon

P.J. Fink Jr.

IBM Thomas J. Watson Research Center, Yorktown Heights, New York 10598

J.W. Schnick

Physics Department, Saint Anselm College, Manchester, New Hampshire 03102

R.H. Landau

Physics Department, Oregon State University, Corvallis, Oregon 97331

(Received 2 January 1990)

Recent $\bar{K}N$ interaction models are used to construct microscopic momentum-space optical potentials including complete Fermi averaging, three-body dynamics, nonlocalities, and the exclusion principle. Bound states are found with \bar{K} orbits internal to and external to the nucleus (Λ^* hypernuclei and kaonic atoms).

I. INTRODUCTION

The low-energy antikaon-nucleon ($\bar{K}N$) interaction possesses interesting complexities from being part of the ($\bar{K}N, \Sigma\pi, \Lambda\pi$) coupled-channels system, and interesting uncertainties and controversies from the scattering and reaction data being so hard to obtain. Supplementary insight into this system is provided by kaonic atoms where the strong interaction modifies what would otherwise be a pure Coulomb state. While measurements of the strong interaction shift of the $1S$ level in kaonic hydrogen¹ would appear to provide valuable direct information on the strong interaction, the difficulties of that experiment has also led to controversy,² with a good number of theorists and experimentalists questioning the results. Consequently, it is logical to look to heavier kaonic atoms where the identification of levels is more reliable than for hydrogen; yet one then has to deal with a challenging many-body problem to interpret the data.³⁻⁷

While as of yet no strong bound state of an antikaon with a nucleus has been observed, since the \bar{K} is known to form a bound state of sorts with individual nucleons [a $\Lambda^*(1405)$ resonance⁸⁻¹¹], it seems possible that nuclear states exist in which a nucleon is replaced by a Λ^* (a Λ^* hypernucleus), or in which a \bar{K} retains its identity and is bound to the entire nucleus. It is unknown whether the nuclear environment causes these nuclear states to be narrow (as it may for Σ hypernuclei^{12,13}), or causes them to be so broad as to have no discernible experimental signal.

In related work, Schnick and Landau^{14,15} recently updated the Alberg *et al.*⁷ potentials for s -wave interactions in the ($\bar{K}N, \Sigma\pi, \Lambda\pi$) system, and found a number of possible solutions. One of these potentials actually provided agreement with both the scattering data and the strong

interaction shift of kaonic hydrogen. While this may be the resolution of a long-standing puzzle, if the hydrogen experiment is incorrect then this particular potential would also be. In follow-up work,¹⁰ the nuclear states of various $\bar{K}N$ interaction models were studied, and it was found that whereas not all potential models supported the Λ^* , some contained multiple resonances at low energies.

In the present paper several of these elementary models are used to construct an optical potential, and the atomic and strong \bar{K} -nucleus bound states are studied. These momentum-space optical potentials include complete Fermi averaging, a three-body model for the energy dependence, dynamic and kinematic nonlocalities, and exclusion principle effects. Since the experimental strong interaction shifts in carbon are probably more reliable than those in hydrogen,¹⁶ this is an important further test of the elementary interactions, and since the optical potential we use has a sounder theoretical basis than is common for this field,¹⁶ we believe this is a meaningful test.

II. BOUND STATES IN MOMENTUM SPACE

Conventional theoretical bound states live forever and occur when the T matrix has a pole at a negative real energy. While actual experimental bound states decay in time, and are thus resonant or Gamow states, they still appear as poles of the T matrix — only now at some complex energy. The real part of the pole's energy is identified with the binding energy E_b , and the imaginary part with the level's width Γ

$$\Gamma = 2\text{Im}E . \quad (1)$$

In our calculation we take the T matrix as the solution of the partial wave Lippmann-Schwinger equation,

$$T_l(k', k; E) = V_l(k', k, E) + \frac{2}{\pi} \int_0^\infty dp p^2 V_l(k', p, E) G_E(p) T_l(p, k; E). \quad (2)$$

Here G is the relativistic Green's function

$$G_E(p) = \frac{1}{E - [\sqrt{p^2 + m_p^2} + \sqrt{p^2 + m_N^2} - (m_p + m_N)]} \quad (3)$$

with E the kinetic energy in the channel under consideration. The Lippmann-Schwinger equation (2) has the formal (operator) solution,

$$T = \frac{1}{1 - VG_E} V = V \frac{1}{1 - G_E V} \quad (4)$$

and so T has poles for energies which satisfy

$$V \approx \langle f | t | i \rangle = A \langle \mathbf{k}', \Psi_o(\mathbf{p}'_1, \mathbf{p}'_2, \dots, \mathbf{p}'_A) | t^{\bar{K}N}(\omega) | \mathbf{k}, \Psi_o(\mathbf{p}_1, \mathbf{p}_2, \dots, \mathbf{p}_A) \rangle \quad (6)$$

where $t^{\bar{K}N}$ is the elementary T matrix, Ψ_o is the nuclear ground state wave function, the \mathbf{p}_i and \mathbf{p}'_i are the momenta of the nucleons in the initial and final nuclear states, and \mathbf{k}' and \mathbf{k} are the \bar{K} 's initial and final momenta. The momenta and wave functions are all in the the \bar{K} -nucleus ($\bar{K}A$) center of momentum (c.m.), and for simplicity of notation we here ignore differences between neutrons and protons. If t is a two-body operator, (6) becomes the explicit integral¹⁷

$$\begin{aligned} V(\mathbf{k}', \mathbf{k}, E) &= A \int d^3p \langle \mathbf{p} - \mathbf{q}, \mathbf{k}' | t^{\bar{K}N}(\omega) | \mathbf{p}, \mathbf{k} \rangle \mathcal{F}(\mathbf{p} - \mathbf{q}, \mathbf{p}), \end{aligned} \quad (7)$$

where \mathcal{F} is the nuclear wave function overlap

$$\begin{aligned} \mathcal{F}(\mathbf{p}' = \mathbf{p} - \mathbf{q}, \mathbf{p}) &= \int d^3p_2 d^3p_3 \dots d^3p_A \Psi_o^*(\mathbf{p} - \mathbf{q}, \mathbf{p}_2, \dots, \mathbf{p}_A), \\ &\times \Psi_o(\mathbf{p}, \mathbf{p}_2, \dots, \mathbf{p}_A) \delta \left(\sum_{i=2}^A \mathbf{p}_i + \mathbf{k} \right), \end{aligned} \quad (8)$$

\mathbf{q} is the momentum transferred to the \bar{K}

$$\mathbf{q} = \mathbf{k}' - \mathbf{k} \quad (9)$$

and the delta function in (8) is the c.m. constraint.

Although simple looking, implementation of (7) re-

$$\det(1 - VG_E) = \det(1 - G_E V) = 0. \quad (5)$$

The linear equations representing these operator relations are obtained by replacing the integrals in (2) and in the representation of (5) by discrete sums over grid points. This is described in some detail in Ref. 15 even for the exceptional Coulomb potential.

III. THEORETICAL OPTICAL POTENTIAL

We start with a $\bar{K}N$ potential or T matrix and use it to construct the theoretical optical potential that describes the multiple scattering of a \bar{K} from the nucleons in a nucleus. We work in momentum space in order to avoid many of the approximations which lessen the validity of the optical potential, and deduce a "potential" quite different from the simple phenomenological ones used in fitting kaonic atom data.¹⁶ We calculate a first order optical potential in impulse approximation,

quires the calculation of a 3D integral for each value of (k, k') on the grid used to solve the Lippmann-Schwinger equation (5), as well as another angular integration for the partial wave projection:

$$V_l(k', k, E) = \int_{-1}^1 V(\mathbf{k}', \mathbf{k}, E) P_l(\cos \theta) d \cos \theta_{kk'}. \quad (10)$$

These 1000's of evaluations of integrals have often been avoided by an optimal factored approximation

$$\begin{aligned} V(\mathbf{k}', \mathbf{k}, E) &\approx A \langle \mathbf{p}_0 - \mathbf{q}, \mathbf{k}' | t^{\bar{K}N}(\omega) | \mathbf{p}_0, \mathbf{k} \rangle \\ &\times \int d^3p \mathcal{F}(\mathbf{p} - \mathbf{q}, \mathbf{p}) \\ &\approx \langle \mathbf{p}_0 - \mathbf{q}, \mathbf{k}' | t^{\bar{K}N}(\omega) | \mathbf{p}_0, \mathbf{k} \rangle F(q), \end{aligned} \quad (11)$$

$$p_0 = -\frac{\mathbf{k}}{A} + \frac{A-1}{2A} \mathbf{q}. \quad (13)$$

This approximation assumes $t^{\bar{K}N}$ is a slowly enough varying function of energy to be factored outside of the integral, with p_0 being the nucleon momentum which optimizes the approximation.¹⁸ Recent advances in computing power has permitted us to evaluate (7) and solve (5) exactly.

A. Fermi integration

We calculate the nuclear overlap function \mathcal{F} by assuming explicit forms for the nuclear wave functions, fitting the corresponding form factor to data, and then using the wave function to calculate \mathcal{F} . We assume ¹²C has neutrons and protons in $\{2(1s), 4(1p_{3/2})\}$ orbitals, and use the $|J, M\rangle$ basis:

$$\phi_1 = |1/2, 1/2\rangle = N_0 e^{-(\alpha^2/2)\mathbf{P}^2} Y_{00} \chi^+ , \quad (14)$$

$$\phi_2 = |1/2, -1/2\rangle = N_0 e^{-(\alpha^2/2)\mathbf{P}^2} Y_{00} \chi^- , \quad (15)$$

$$\phi_3 = |3/2, 3/2\rangle = N_1 \alpha p e^{-(\alpha^2/2)\mathbf{P}^2} Y_{11} \chi^+ , \quad (16)$$

$$\phi_4 = |3/2, 1/2\rangle = N_1 \alpha p e^{-(\alpha^2/2)\mathbf{P}^2} (\sqrt{1/3} Y_{11} \chi^- + \sqrt{2/3} Y_{10} \chi^+) , \quad (17)$$

$$\phi_5 = |3/2, -1/2\rangle = N_1 \alpha p e^{-(\alpha^2/2)\mathbf{P}^2} (\sqrt{2/3} Y_{10} \chi^- + \sqrt{1/3} Y_{1-1} \chi^+) , \quad (18)$$

$$\phi_6 = |3/2, -3/2\rangle = N_1 \alpha p e^{-(\alpha^2/2)\mathbf{P}^2} Y_{1-1} \chi^- . \quad (19)$$

The total wave function $\Psi(p_1, p_2, \dots, p_Z)$ for the Z protons is the antisymmetric combination

$$\Psi(p_1, p_2, \dots, p_Z) = \frac{1}{\sqrt{Z!}} \begin{vmatrix} \phi_1(p_1) & \phi_2(p_1) & \cdots & \phi_Z(p_1) \\ \phi_1(p_2) & \phi_2(p_2) & \cdots & \phi_Z(p_2) \\ \vdots & \vdots & \ddots & \vdots \\ \phi_1(p_Z) & \phi_2(p_Z) & \cdots & \phi_Z(p_Z) \end{vmatrix} . \quad (20)$$

This determinantal form for Ψ simplifies the integration in (8) since the orthogonality of the eigenfunctions eliminates the cross terms resulting in

$$\begin{aligned} Z\mathcal{F}(\mathbf{P}', \mathbf{p}) &= \frac{2N_0^2}{4\pi} e^{-(\alpha_0^2/2)(\mathbf{P}')^2} e^{-(\alpha_0^2/2)\mathbf{P}^2} \\ &\quad + 4/3 N_1^2 \alpha_1 e^{-(\alpha_1^2/2)(\mathbf{P}')^2} e^{-(\alpha_1^2/2)\mathbf{P}^2} \left[p' Y_{10}^*(\hat{\mathbf{p}}') p Y_{10}(\hat{\mathbf{p}}) + p' Y_{11}^*(\hat{\mathbf{p}}') p Y_{11}(\hat{\mathbf{p}}) + p' Y_{1-1}^*(\hat{\mathbf{p}}') p Y_{1-1}(\hat{\mathbf{p}}) \right] , \end{aligned} \quad (21)$$

$$= \frac{1}{Z} \left(\frac{2}{\sqrt{\pi}} \right)^3 \left[Z_0 \alpha_0^3 e^{-\alpha_0^2 p'^2/2} e^{-\alpha_0^2 p^2/2} + 2/3 Z_1 \alpha_1^3 [\alpha_1^2 \mathbf{p} \cdot \mathbf{p}'] e^{-\alpha_1^2/2 \mathbf{p} \cdot \mathbf{p}'} e^{-\alpha_1^2 p'^2/2} \right] , \quad (22)$$

where we allow different sizes α_0 and α_1 for the s and p shells. In Cartesian coordinates (in which the integration is most straight forward), \mathcal{F} takes the form

$$\mathcal{F}(\mathbf{P}', \mathbf{p}) = \frac{1}{Z} \left[Z_0 \left(2 \frac{\alpha_0}{\sqrt{\pi}} \right)^3 e^{-\alpha_0^2(\zeta_x^2 + \zeta_y^2 + \zeta_z^2)} e^{-\alpha_0^2/4 q^2} + 2/3 Z_1 \left(2 \frac{\alpha_1}{\sqrt{\pi}} \right)^3 \alpha_1^2 \sum_{i=1}^3 (\zeta_i^2 - q_i^2/4) e^{-\alpha_1^2(\zeta_x^2 + \zeta_y^2 + \zeta_z^2)} e^{-\alpha_1^2/4 q^2} \right] , \quad (23)$$

$$\zeta_i \equiv p_i - q_i/2 = \frac{p_i + p'_i}{2} , \quad (24)$$

where Z_0 and Z_1 are the number of protons in the $1s$ and $1p$ shells (2 and 4 for carbon).

Equation (23) provides an algebraic form for the overlap function. Since Eq. (12) determines the corresponding form factor to be

$$F(q) = \frac{1}{Z_0 + Z_1} \left[Z_0 e^{-\alpha_0^2 q^2/4} + Z_1 \left(1 - \frac{\alpha_1^2 q^2}{6} \right) e^{-\alpha_1^2 q^2/4} \right] . \quad (25)$$

we determined the parameters $(\alpha_0, \alpha_1) = (1.526, 1.626)$ fm by fitting F to fits to electron scattering data.¹⁹ We assume neutrons and protons have the same matter distribution, namely the charge form factor with the nucleon form factor removed^{21,22}:

$$F_{\text{mat}}(q) = \frac{F_{\text{ch}}(q)}{f(q)} = F_{\text{ch}}(q)(1 + q^2/18.2 \text{ fm}^{-2})^2 . \quad (26)$$

B. Three-body energy

The t in the optical potential describes a \bar{K} scattering from a nucleon which in turn is interacting with the other nucleons in the nucleus. We assume the ‘‘impulse approximation’’ to ignore the binding effects which would otherwise require solution of the $A+1$ body problem, but choose the $\bar{K}N$ subenergy ω to be the ‘‘3-body energy’’ ω_{3B} in order to include binding effects in a simpler way. As shown in Fig. 1, in the $\bar{K}A$ c.m., the nucleus is viewed as an active nucleon of momentum $\mathbf{p} + \mathbf{p}_0$ external to a passive core of momentum

$$\mathbf{P} = -\mathbf{k} - \mathbf{p} - \mathbf{p}_0 . \quad (27)$$

The subenergy is then the magnitude of the difference of the four-momentums of the kaon+nucleus and core:

$$\omega_{3B}^2 = (k_K^\mu + k_A^\mu - P^\mu)^2 . \quad (28)$$

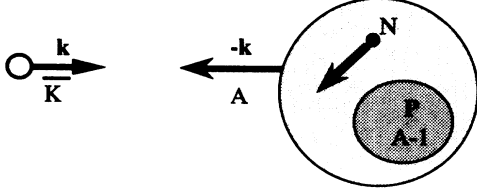


FIG. 1. The three-body model of the optical potential, a \bar{K} of momentum \mathbf{k} interacting with a nucleon bound to a passive core of momentum \mathbf{P} .

To follow this model properly would require solving a full three-body problem including the effect of the core-nucleon potential V_{CN} . We avoid that by replacing $p^2/2m + V_{CN}$ with its expectation value E_B , an effective core-nucleon binding energy,

$$E_B = \langle p^2/2m + V_{CN} \rangle, \quad (29)$$

$$\omega_{3B}^2 \approx [E_K(k_0) + E_A(k_0) - E_{A-1}(P) - E_B]^2 - P^2. \quad (30)$$

When the $\bar{K}N$ T matrix is averaged over the nucleon's internal momentum, the subenergy varies over the range $-\infty \leq \omega_{3B} \leq K_{\text{inc}} - E_B$, where K_{inc} is the incident kinetic energy of the kaon (negative for bound states). Thus the subtractions in (30) make the effective $\bar{K}N$ kinetic energy predominantly negative.²⁰ For single-channel scattering, this means the elementary T matrix (and thus the first-order optical potential) become real at low energy — which makes good physical sense since it means the absorption arising from nucleon knockout ceases when there is not enough energy to knock out a nucleon. For the present calculation, we describe bound processes which never have enough energy for nucleon knockout, in which case absorption arises from shadows in the $\bar{K}N$ T matrix of the open $\Sigma\pi$ and $\Lambda\pi$ channels. Consequently, even though the elementary t 's are evaluated at negative kinetic energies, they have imaginary parts that cause all nuclear bound states to be unstable.

C. Covariant momenta

The t in the optical potential must be evaluated in the $\bar{K}A$ c.m.. There is a good deal of technology involved in finding the best way to relate the t 's in the different frames, and we refer the interested readers to Refs. 18 for details. We generalize the on-energy-shell Lorentz invariance of probability to off shell scattering by relating $t^{\bar{K}N}$ in the kaon-nucleus c.m. to \tilde{t} in the $\bar{K}N$ c.m. via

$$\langle \mathbf{k}', \mathbf{p}' | t^{\bar{K}N}(\omega) | \mathbf{k}, \mathbf{p} \rangle = \gamma \langle \mathbf{k}' | \tilde{t}(\omega) | \mathbf{k} \rangle \quad (31)$$

$$\gamma = \left[\frac{E_p(\kappa) E_p(\kappa') E_n(\kappa) E_n(\kappa')}{E_p(k) E_p(k') E_n(p) E_n(p')} \right]^{1/2} \quad (32)$$

where γ arises from conservation of probability. The initial and final $\bar{K}N$ c.m. momenta κ and κ' are related to those in the $\bar{K}A$ c.m. via the “magic-vector angle transformation”

$$\kappa = \mathbf{Q} - \frac{\mathbf{Q} \cdot \mathbf{K}}{K_0(K_0 + \sqrt{s_{\text{in}}})} \mathbf{K}, \quad (33)$$

$$2\mathbf{Q} = \mathbf{k} - \mathbf{p}_0 - \frac{m_K^2 - m_N^2}{s_{\text{in}}} \mathbf{K}, \quad s_{\text{in}} = (p^\mu + k^\mu)^2, \quad (34)$$

$$K = (K_0, \mathbf{K}) = (E_K(k) + E_N(p), \mathbf{k} + \mathbf{p}) \quad (35)$$

with equivalent definitions for κ' . Eqs. (33)–(35) are unique prescriptions if covariance is demanded in an on-mass-shell theory.

The off-energy-shell $\bar{K}N$ T matrix $\langle \mathbf{k}' | \tilde{t}(\omega) | \mathbf{k} \rangle$ in (31) is obtained by solving coupled Lippmann-Schwinger integral equations for the $(\bar{K}N, \Sigma\pi, \Lambda\pi)$ coupled channels.¹⁵ In this way we maintain an important internal consistency by using the same form for the Green's function in the two- and many-body problems. Since the on-shell $\bar{K}N$ t 's have been fit to the scattering and reaction data, examining bound state data provides a supplementary test; the scattering data are sensitive to the $\bar{K}N$ wave function in the large r region, while the bound states are sensitive to smaller r values.

D. Exclusion principle

The exclusion principle forbids a recoiling nucleon from entering into a state already occupied by another nucleon — and thus has no effect upon a \bar{K} or Λ^* (unless the quarks' bags dissolve in a nucleus). While some exclusion is present in the overlap function \mathcal{F} Eq. (8) derived from a determinantal wave function, we also incorporate it in the elementary $t^{\bar{K}N}$ by including an operator Q into the $\bar{K}N$ Lippmann-Schwinger equation which permits only unoccupied intermediate nucleon states:

$$\begin{aligned} \langle \mathbf{k}' | \tilde{t}(\omega) | \mathbf{k} \rangle &= \langle \mathbf{k}' | \tilde{v} | \mathbf{k} \rangle \\ &+ \int d^3p \frac{\langle \mathbf{k}' | \tilde{v} | \mathbf{p} \rangle Q(\mathbf{p}) \langle \mathbf{p} | \tilde{t}(\omega) | \mathbf{k} \rangle}{\omega - \omega(\mathbf{p}) + i\epsilon} \end{aligned} \quad (36)$$

Since Q depends on the nuclear wavefunctions, we are including nonlinear nuclear density dependences into the optical potential.

Although it would be better to determine Q from determinantal wave functions, we keep the computation simpler by using the Fermi gas model

$$Q(p) = \begin{cases} 0 & \text{if } p_N < p_F \\ 1 & \text{if } p_N > p_F \end{cases}, \quad (37)$$

where p_N is the momentum of the nucleon relative to the nuclear c.m.. We relate p_N to the $\bar{K}N$ relative momentum κ and the $\bar{K}N$ total momentum K (and remove some of the harshness of this model) by taking an average

over scattering angle (standard for nuclear structure)

$$Q(K, \kappa) = \begin{cases} 0 & \text{if } \chi K + \kappa < p_F \\ 1 & \text{if } |\chi K - \kappa| > p_F \\ \frac{(\chi K + \kappa)^2 - p_F^2}{4\chi K \kappa} & \text{otherwise} \end{cases}, \quad (38)$$

$$\chi \equiv \frac{m_N}{m_p + m_N}, \quad p_F = \left(\frac{3\pi^2}{2} \rho \right)^{1/3}. \quad (39)$$

When searching for *nuclear* states, we assume the \bar{K} orbits deep within the nucleus, in which case the appropriate r for ρ is for the nuclear interior, and thus obtain $p_F = 260 \text{ MeV}/c$. When searching for the *atomic* states, we assume the \bar{K} is in a Bohr-like orbit, in which case the appropriate r for ρ is the one in which there is maximum overlap of the Coulomb wave function and the nuclear density, and thus obtain $p_F = 140 \text{ MeV}/c$.

IV. ATOMIC RESULTS

To set the scale, in Fig. 2 we show the relative sizes of the Bohr radii

$$R_B = \frac{\hbar c}{Z\alpha\mu c^2} n^2 \quad (40)$$

of the $1S$ level in kaonic hydrogen, the $2P$ levels in kaonic ${}^4\text{He}$ and ${}^{12}\text{C}$, and the radius of the carbon nucleus itself. Since the \bar{K} in carbon is closest to the nucleus yet still far outside of it, we expect this level to be shifted most

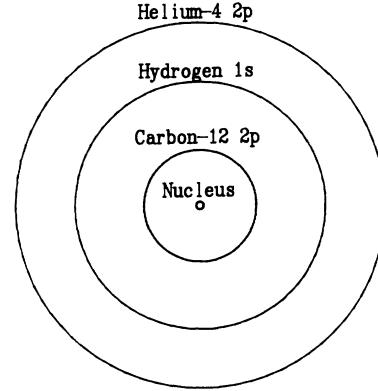


FIG. 2. The relative sizes of the Bohr orbits for a K^- in ${}^{12}\text{C}$, H, and ${}^4\text{He}$, and for the carbon nucleus.

by the nuclear force (it is) — but wonder if it is close enough to the nucleus to probe the small r $\bar{K}N$ interaction. If this latter (off-energy shell) sensitivity exists, the strong interaction shift will differ for various models of the elementary interaction, and kaonic atoms can be used to distinguish among them.

A. Sign of shift

The previous study¹⁵ took a number of elementary potentials, calculated exactly the $1S$ energy of kaonic hydrogen, and compared these results to the experimental shift and width¹

$$(\epsilon, \Gamma)_H^{\text{exp}} = (40 \pm 60, 0 + 230), (264 \pm 76, 544 \pm 356), (200 \pm 60, 80_{-80}^{+220}) \text{ eV}. \quad (41)$$

(Positive ϵ means the strong interaction shifts the Coulomb level towards the *more* bound.) A significant off-shell sensitivity was found, with r_2 , the only potential to agree with the *positive* sign of ϵ , also agreeing with its magnitude.

Since the $2P$ orbit in carbon has a greater nuclear overlap than the $1S$ level in hydrogen, if we were in the perturbative regime we might expect it to have a greater sensitivity to the elementary interaction. Yet since the carbon potential is strongly absorptive and attractive, its shift is subject to Krell-Seki oscillations,^{3,4} and so its relative size and sign is hard to know offhand.

We have taken each elementary interaction determined by Ref. 15, built an optical potential with it, added in the Coulomb potential, and calculated exactly the energy of the $2P$ level in kaonic carbon. In Figs. 3 and 4 we show the predicted shifts and widths along with the experimental data of Backenstoss *et al.*²³

$$(\epsilon, \Gamma)_C^{\text{exp}} = (-590 \pm 80, 173 \pm 150) \text{ eV}. \quad (42)$$

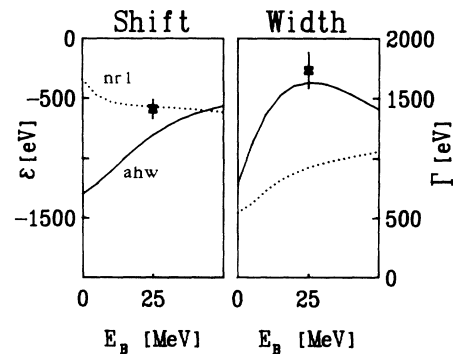


FIG. 3. The strong interaction shift and width of the $2P$ level of kaonic ${}^{12}\text{C}$ as a function of the effective nucleon binding energy E_B in the model of Fig. 1. The two curves are calculated with optical potentials based on AHW (solid curve) and nr1 (dashed curve) elementary interactions. The data are from Backenstoss *et al.*²³

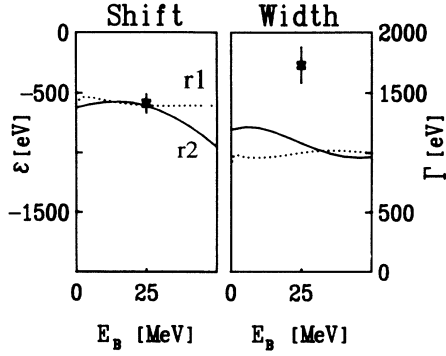


FIG. 4. The same as Fig. 2 only here for optical potentials based on the elementary interactions r1 (dashed curve) and r2 (solid curve).

We note that the *experimental* shift and width in carbon are much larger in magnitude than those of hydrogen (with the latter results questioned by many), Eq. (41), with the negative shift in carbon (to the *less* bound) of opposite sign to that in hydrogen. We next note that the potentials shown in Figs. 3 and 4 predict a negative shift towards the *less* bound — even r2 which agreed with the data in hydrogen by predicting a shift towards the *more* bound. To explain this we refer to Fig. 5 which shows the k^-p scattering amplitude for models r1 and r2 (the “r” denotes relativistic kinematics). We see that r1’s amplitude displays a conventional Λ^* resonance near 1400 MeV: $\text{Im}f$ peaks and $\text{Re}f$ changes sign. In contrast, r2’s amplitude does not manifest a resonance signal: its real part does not change sign and is positive at the k^-p

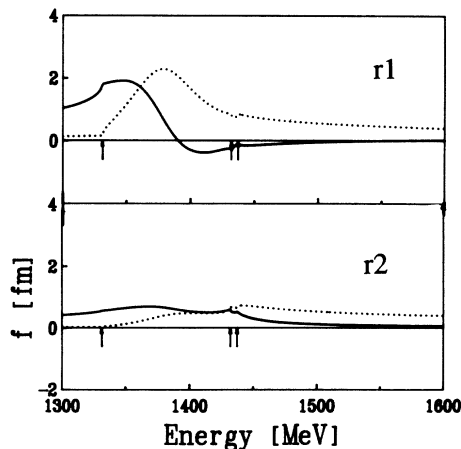


FIG. 5. Real and imaginary parts (solid and dotted curves) of the K^-p elastic scattering amplitude for the relativistic potentials r2 and r1. Arrows point to threshold energies.

threshold at 1432 MeV (it does however contain a resonance in the $\Sigma\pi$ channel). Consequently, r2 predicted a *positive* shift for kaonic hydrogen whereas r1 and the other models predicted a negative shift.

When these elementary amplitudes are used in the optical potential, they are evaluated at the three-body energy (30), which means the nucleon’s Fermi motion and recoil cause them to be evaluated at energies considerably below threshold. This in turn means all amplitudes have the same (positive) sign for their real parts, and thus all predict the same (negative) sign for the shift. Yet this also means that although all real parts of the optical potentials are attractive, they all shift the Coulomb bound state towards the less bound. This is not a contradiction but rather the property of strongly-absorptive potentials we referred to earlier as the Krell-Seki oscillation. On a more microscopic level it is explained by the existence of an odd number of strongly bound states within the nucleus³ — a possibility we explore in Sec. V.

B. Model Dependence

Returning to Figs. 3, we note the complex shifts produced by optical potentials based on the two-body interactions with nonrelativistic kinematics, AHW (Ref. 7) and nr1 (Ref. 15’s update of AHW), and in Fig. 4 with potentials based on the relativistic interactions r1 and r2. The agreement for the r2-based optical potential is important since r2 is the only interaction to also agree with the kaonic hydrogen experiments (which future experiments may well prove to be in error). The curves show the dependence of the shift on the effective, nucleon binding energy E_B of Eq. (30). For $E_B \approx 25$ MeV all potentials agree reasonably well with the shift ϵ . In general there is also somewhat too small a width predicted, a trend also found by Alberg *et al.*⁷ in their coordinate-space study.

Not shown here are the predictions for optical potentials constructed from the elementary, nonrelativistic interactions nr2 and nr3. Their agreements with the carbon data are significantly poorer, and so we eliminate them as viable elementary interactions. This is interesting since it shows that even though nr2 was the best nonrelativistic fit to the low energy two-body scattering data, the nuclear bound state energy is an independent and rigorous test. Potential nr3, on the other hand, did not show a definite resonance signal in any channel, in which case it is satisfying to see the carbon data rule it out.

V. HYPERNUCLEAR RESULTS

By searching for complex energies which are solutions of Eq. (5), $\det[1 - G_E U(E)] = 0$, we have studied if the optical potentials describing kaonic carbon also support deeply bound, nuclear states (hypernuclei in which a nucleon converts to a Λ^* or a \bar{K} binds to the nucleus). The search requires numerous evaluations of the deter-

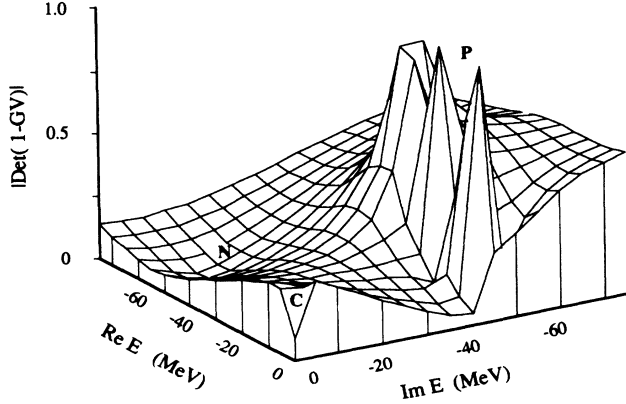


FIG. 6. The magnitude of the $\det(1 - GV)$ as a function of the complex energy for an optical potential using the r2 interaction in factored approximation. The point N marks the nuclear bound state, C the Coulomb states, and P the potential poles.

minant of a complex matrix, each evaluation requiring the optical potential matrix on a large grid, with each matrix element requiring a four-dimensional integration over the solution of a coupled-channels integral equation. Further, in order to know in which direction to search, numerous evaluations of the gradient of $\det[1 - G_E U(E)]$ are required.

The difficulty of this study is evidenced by the plot in Fig. 6 of $\det[1 - G_E U(E)]$ vs complex energy for an r2-based optical potential in factored approximation. A hypernuclear state occurs as the zero of the determinant, and is seen as the broad dip near $(-50 - 10i)$ MeV. The atomic, Bohr-like states are all squeezed into the steep hole near the origin. The spikes (and the zeros between them) are poles in the determinant arising from poles in the optical potential itself [which in turn originate from a pole in the $\bar{K}N t$ matrix at a $\bar{K}N$ c.m. energy of $(-52, -39)$ MeV, Ref. 10]. These spikes are sharp enough for the gradient not to be well defined near them, which foils our search routine.

A. Binding energies

$\bar{K}C$ hypernuclear binding energies are given in Table I for optical potentials constructed with full Fermi averaging (7) and in factored approximation (12). Also listed in the last column are the pole positions for the elementary

K^-p amplitude. We see that for both potentials the full integration makes the S -wave states some 20% less bound and narrower. Further, for the r2-based optical potential, the nuclear environment *narrows* the width of the elementary state by a factor of 4, but *increases* its binding only slightly. For the AHW-based potential, the nuclear environment *broadens* the width by nearly a factor of 2, and *increases* its binding by a factor of 4. We suspect the different behaviors arise from having a strongly absorptive optical potential — which is known to be sensitive to even small changes, and from having two elementary interactions with widely differing ranges¹⁵:

$$\beta_0^{-1}(r2, \text{AHW}) = (0.092, 0.180) \text{ fm} \quad (43)$$

Also given in Table I are energies of the first P -wave hypernuclear state (the finite nuclear size induces P waves from the elementary s waves). We see that the P wave states are less bound, and that one of them which existed in the factored approximation no longer exists with full Fermi averaging (possibly it is shifted to a region we did not explore).

B. Model dependence

The dependence of the hypernuclear energies upon the effective nucleon binding energy E_B is similar in the factored approximation (11) and full integration (7), as well as similar for the different input potentials. As we see in Fig. 7, the complex hypernuclear binding energy E_h varies relatively slowly with E_B — as least when compared to the atomic binding energy dependence in Fig. 3. Although the $\bar{K}N T$ matrix is a rapidly varying function of energy near threshold, the momentum dependent terms in the three-body energy (30) shift the effective $\bar{K}N$ subenergy down to a region below threshold, and here T is a smooth function of energy.

The dependence of E_h upon p_F is similar for factored and nonfactored approximations. Whereas the inclusion of exclusion into the elementary amplitudes has little effect for atomic states, there is more sensitivity for hypernuclear states. Since increasing p_F blocks out more of the final states available to the recoiling nucleon, this reduces the strength of the $\bar{K}N T$ matrix [and especially that of the imaginary part since it arises from the intermediate state in (36)]. However, since the potential is too strong for there to be a simple relation between binding energy and potential strength, it is hard to predict how this reduction affects the hypernuclear binding

TABLE I. Complex binding energies in MeV for $\bar{K}^{12}\text{C}$.

$\bar{K}N$ Potential Input	$E_h (l=0)$	$E_h (l=1)$	E_{K-p}
r2 (full)	-46 -9.i	not found	
r2 (factored)	-53 -11i	-9. -27i	-52 -39i
AHW (full)	-61 -42i	-10 -31i	
AHW (factored)	-67 -54i	-17 -37i	-14 -25i

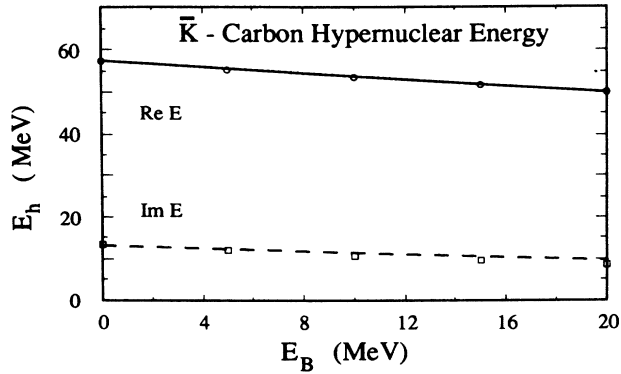


FIG. 7. The real and imaginary parts (solid and dashed curves) of the Λ^* hypernuclear binding energy E_h as a function of the effective nucleon binding energy E_B . The optical potential uses the r2 elementary interaction in nonfactored approximation.

energy. In general, the dependence is less than the E_B dependence shown in Fig. 7.

VI. SUMMARY AND CONCLUSIONS

In this, the last of a three-paper series, we have embedded the elementary coupled-channels $\bar{K}N$ interactions deduced in paper 1 (Refs. 14 and 15) into a many-body environment. This extends the testing of the interactions from scattering, reactions, and kaonic hydrogen, into kaonic carbon. Here we also tested if the strong bound states found to exist with the elementary interactions in paper 2 (Ref. 10) continue to exist in the nuclear environment, and if so, how they are modified. Our studies are conducted with an optical potential including full Fermi averaging, an important consideration for an interaction with a strong energy dependence.

We find that several elementary interactions predict a strong interaction shift of the $2P$ level in kaonic carbon in agreement with experiment (to the less bound). In particular, the interaction r2 (the only one to predict the

experimental shift to the more bound in hydrogen) generates an optical potential in agreement with kaonic carbon. The predicted widths in carbon are smaller than experiment, and we suspect agreement may require a more accurate, coupled-channels optical potential.

A single strong bound state (Λ^* hypernuclei) for both S and P waves in carbon was found for each elementary interaction. This is not too surprising since strong states exist in the coupled-channels elementary interaction — yet since in the nuclear case there is strong absorption, and since our optical potential is a single channel model, their discovery was not certain. The existence and energy levels of these states provide further insight into the nature of the $\Lambda_0^*(1405)$ resonance. The hypernuclear state exists for a number of models and optical potential parameters, although its binding energy of course varies. For our best model, r2 with full Fermi averaging, the state is bound by 46 MeV with a width of 18 MeV. Its best experimental signal may be a peaking of energy in one of the Λ^* decay channels.

Our general conclusion is that the theoretical optical potential appears to be a reasonably sensitive testing ground for models of elementary interactions, both potential and quark models. Further nuclei should clearly be investigated. A needed extension to the present work is a coupled-channels optical potential which would include the structure of nuclei in which one of the nucleons has turned into either a Λ or a Σ , and would thus relate a number of hypernuclear species.

ACKNOWLEDGMENTS

We wish to thank Byron Jennings, A.W. Thomas, M. Alberg, G. He, and L. Willets for stimulating and illuminating discussions. Support from the Department of Energy and the IBM Corporation is gratefully acknowledged and appreciated. One of us (R.H.L.) would also like to thank the good people at The University of Adelaide and Melbourne Physics Departments, and at The T.J. Watson Research Center of IBM for their support and hospitality during his visits.

¹J. D. Davies, G. J. Pyle, G. T. A. Squier, C. J. Batty, S. F. Biagi, S. D. Hoath, P. Sharman, and A. S. Clough, *Phys. Lett.* **83B**, 55 (1979); M. Izycki, G. Backenstoss, L. Tauscher, P. Blüm, R. Guigas, N. Hassler, H. Koch, H. Poth, K. Fransson, A. Nilsson, P. Pavlopoulos, and K. Zioutas, *Z. Phys. A* **297**, 11 (1980); P.M. Bird, A.S. Clough, K.R. Parker, G.J. Pyle, G.T.A. Squier, S. Baird, C.J. Batty, A.I. Kilvington, F.M. Russell, and P. Sharman, *Nucl. Phys.* **A404**, 482 (1983).

²K.S. Kumar, Y. Nogami, W. van Dijk, and D. Kiang, *Z. Phys. A* **304**, 301 (1982); K.S. Kumar and Y. Nogami, *Phys. Rev. D* **21**, 1834 (1980).

³J.H. Koch, M.M. Sternheim, and J.F. Walker, *Phys. Rev. Lett.* **26**, 1465 (1971); *Phys. Rev. C* **5**, 381 (1972).

⁴R.Seki, *Phys. Rev. C* **5**, 1196 (1972).

⁵W. A. Bardeen and E. W. Torogoe, *Phys. Lett.* **38B**, 135 (1972).

⁶R. Staronski and S. Wycech, *Czech. J. Phys. B* **36**, 903 (1986).

⁷M. Alberg, E. M. Henley, and L. Willets, *Ann. Phys.* **96**, 43 (1976).

⁸E. A. Veit, B. K. Jennings, A. W. Thomas, and R. C. Barrett, *Phys. Rev. D* **31**, 1033 (1985).

⁹B.K. Jennings, *Phys. Lett.* **176B**, 229 (1986).

¹⁰P.J. Fink, Jr., G. He, R.H. Landau, and J.W. Schnick, "Bound States, Resonances, and Poles in Low-Energy $\bar{K}N$ Interaction Models," Oregon State University report, 1989.

¹¹R.H. Dalitz and J.G. McGinley, in *Low and Intermediate Energy Kaon-Nucleon Physics*, edited by E. Ferrari and G. Violini, (Reidel, Boston, 1981), p. 97; R.H. Dalitz,

- J. McGinley, C. Belyea, and S. Anthony, *Proceedings of the International Conference on Hypernuclear and Kaon Physics, Heidelberg, 1982* (Max-Planck-Institut für Kernphysik, Heidelberg, 1982), p. 201.
- ¹²J.A. Johnstone and A.W. Thomas, Nucl. Phys. **A392**, 409 (1983).
- ¹³A. Gal, G. Toker, and Y. Alexander, Ann. Phys. (N.Y.) **136**, 341 (1981).
- ¹⁴J.W. Schnick and R.H. Landau, Phys. Rev. Lett. **58**, 1719 (1987).
- ¹⁵J.W. Schnick and R.H. Landau, "Potential Models for Low-Energy $\bar{K}N$ Scattering, Reactions, and Atoms," Oregon State University report, 1989.
- ¹⁶C.J. Batty, Light Kaonic and Antiprotonic Atoms, *Twelfth International Conference on Few Body Problems in Physics*, Vancouver, British Columbia, 1989, edited by H. W. Fearing [Nucl. Phys. **A508**, 89 (1990)]; *Proceedings of the International Conference on Hypernuclear and Kaon Physics, Heidelberg, 1982*, edited by B. Pouh (Max-Planck-Institut für Kernphysik, Heidelberg, 1982), p. 297.
- ¹⁷A. K. Kerman, H. McManus, and R. M. Thaler, Ann. Phys. **8**, 551 (1959).
- ¹⁸A.W. Thomas and R.H. Landau, Phys. Rep. **58**, 121 (1980); Nucl. Phys. **A302**, 461 (1978).
- ¹⁹J. L. Friar and J. W. Negele, Nuc. Phys. **A240**, 93 (1975).
- ²⁰The shift is not a simple evaluation of t at a lower energy: the momenta variables are not shifted (this is *off-shell* scattering) whereas the shift depends upon k and k' .
- ²¹B. Bartoli, F. Felicetti, and V. S. Silvestrini, Rev. Nuovo Cimento **2**, 241 (1972).
- ²²The meson exchange currents of the electromagnetic form factors are inappropriate for the optical potential, yet we ignore their effect on bound states since they are significant only at very large momentum transfers.
- ²³G. Backenstoss, J. Egger, H. Koch, H. P. Povel, A. Schwit-ter, and L. Tauscher, Nucl. Phys. **B73**, 189, (1974).

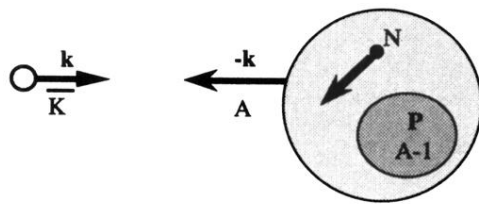


FIG. 1. The three-body model of the optical potential, a \bar{K} of momentum \mathbf{k} interacting with a nucleon bound to a passive core of momentum \mathbf{P} .